Experimental Separation of Photoabsorption and Compton Scattering Contributions to He Single and Double Ionization

L. Spielberger*, O.Jagutzki, R. Dörner, J. Ullrich+, U. Meyer, V. Mergel, M. Unverzagt, M. Damrau, T. Vogt, I. Ali, Kh. Khayyat, D. Bahr‡, H.G. Schmidt‡, R. Frahm‡, and H. Schmidt-Böcking

Institut für Kernphysik, Universität Frankfurt, D60486 Frankfurt/M., Germany,
+ GSI, D64220 Darmstadt, Germany, *‡ HASYLAB am DESY, D22603 Hamburg, Germany*

We have experimentally separated the contributions of photoabsorption and Compton scattering to He single and double ionization for high-energy photon impact by measuring the full momentum vector of the recoiling $He^{1+,2+}$ ions. For recoil ions following photoabsorption large momenta and a distinct dipole emission pattern are observed. The ions produced by Compton scattering show small momenta. For the ratio of double to single ionization we find $(1.22 \pm .06)\%$ at $8.8^{+1.5}_{-1.65}$keV for Compton scattering and $(1.72 \pm .12)\%$ at $7.0^{+2.1}_{-1.6}$keV for photoabsorption. We compare our data with recent theories.

INTRODUCTION

The interaction of a photon with an atom is described by a single particle operator. Thus double ionization is always mediated by electron–electron correlation. Therefore the description of He double ionization induced by photons is one of the most crucial tests of our understanding of these correlation effects. At small photon energies below 1 keV considerable success has been achieved in the realization of kinematical complete experiments and their theoretical description [1–3]. At these low energies absorption of the photon is the dominating ionization mechanism. In the high energy regime (above about 8 keV) Compton scattering is the leading process, the respective single ionization cross sections getting equal around 6 keV photon energy [4–8].

In the high-energy regime even the ratio of total cross sections for double to single ionization ($R = \sigma^{2+}/\sigma^{1+}$), which is predicted to converge with increasing energy to a constant value, is not yet well established [9]: Only a few experimental results on R have been reported [10,11]. Unfortunately these experiments were not able to distinguish between photoabsorption and Compton scattering. From the theoretical side agreement has been achieved [12] in predicting the asymptotical value for R_{Ph} to be 1.67% [13–15,4]. For Compton scattering different theoretical predictions for the high-energy limit as well as for the energy dependence of R_C exist [8,12,16]. At 8 keV, where the present experiments were performed, the predictions for R_C differ by more than a factor of two between 0.6% [8], 1.3% [12] and 1.65% [7].

Here we present an experimental approach which allows to distinguish both ionization mechanisms. Since ions from Compton events and photoionization

are distinct in momentum space measuring the recoil momentum vector of the ions simultaneously with their charge state provides for the first time a separate determination of the ratios R_C and R_{Ph}. We present these ratios determined at a photon energy of about 8 keV. We find a close connection between the Compton profile [17] and the single ionization recoil ion momentum distribution at low momenta.

EXPERIMENT

In order to determine R_{Ph} and R_C separately not only the recoil ion charge state but also the recoil ion momentum was measured in the present experiment using COLTRIMS (COLd Target Recoil Ion Momentum Spectroscopy). The apparatus used is described in detail elsewhere [18–20]. It consists of a supersonic He gas jet, that provides a dense, localized and internally cold He target. The recoiling He ions created in the intersection volume of photon beam and target jet are extracted by a well defined homogeneous electrostatic field onto a position sensitive detector. Since *all* ions are projected on the detector the full 4π solid angle is obtained for both He charge states. The gas jet atoms have an offset momentum of 6 a.u. in y direction resulting from the supersonic expansion. The internal momentum spread of the target is below 0.2 a.u., which corresponds to a temperature below 0.1 K. The ion time of flight (TOF) is determined by measuring their timing signal with respect to the beam pulse provided from the storage ring. From the TOF we obtain the recoil ion charge state and the momentum component parallel to the field direction. The two momentum components perpendicular to the extraction field are calculated from the position on the channel-plate detector (see FIG. 1) and the TOF.

The experiment has been performed at the undulator beamline BW1 of HASYLAB at DESY in Hamburg. Two experiments have been carried out at the same time at this beamline. The main experiment used a small band pass of x-rays reflected out of the direct beam by a Be single crystal monochromator of 0.25 mm thickness operated in Laue transmission geometry. Our experiment was performed with all photons passing in forward direction through the Be crystal. Thus, the radiation used in this experiment was not monoenergetic. The photon spectrum is shown in FIG. 0.2. It was measured after the experiment with a Si (111) single crystal in $\Theta - 2\Theta$ geometry. The spectrum is dominated by the third harmonic of the undulator which was set to 9.2 keV. It is cut below 5 keV by the absorption of the beam line windows (Carbon, Beryllium, and Aluminium) and the Be crystal, and on the high energy side at about 11 keV by two Au coated mirrors. These mirrors were used to focus the light in the vertical and horizontal direction. A beamspot of less than 1×2 mm was achieved by two sets of adjustable slits about 1 and 1.5 m upstream the collision region. The experiment was performed at a flux of about 1×10^{14} photons/sec over the whole spectrum yielding about 80 He^{1+} ions/sec.

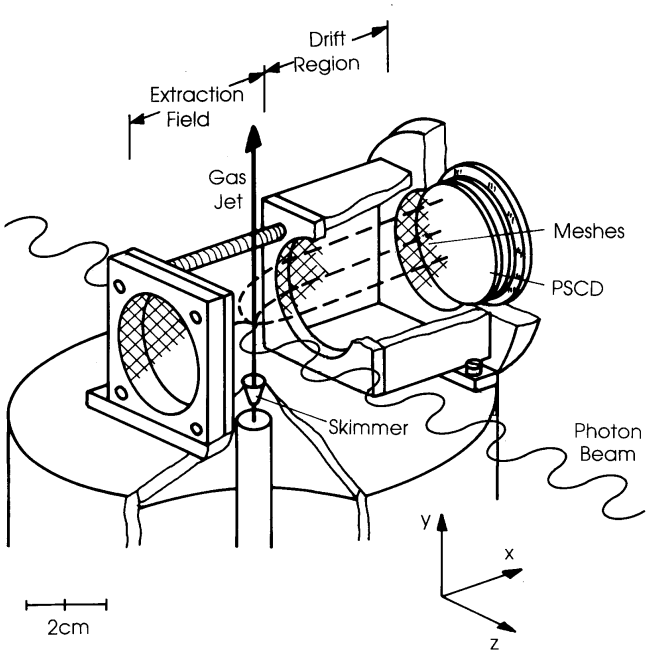

FIGURE 0.1 Recoil-ion momentum spectrometer with supersonic He gas jet. The recoil ions have been measured in coincidence with the beam pulse, the channel-plate detector (PSCD) is two dimensional position sensitive with wedge and strip readout. The electric field vector of the linear polarized light is parallel to the extraction field.

REMARKS ON THE RECOIL ION KINEMATICS

The momentum balances for the different reactions investigated are:

$$\begin{aligned}
\vec{p}_\gamma + \vec{p}_{\mathrm{He}} &= \vec{p}_{\mathrm{He}^{1+}} + \vec{p}_{\mathrm{e}} && (\text{Photo, } \mathrm{He}^{1+}) \\
\vec{p}_\gamma + \vec{p}_{\mathrm{He}} &= \vec{p}_{\mathrm{He}^{2+}} + \vec{p}_{\mathrm{e1}} + \vec{p}_{\mathrm{e2}} && (\text{Photo, } \mathrm{He}^{2+}) \\
\vec{p}_\gamma + \vec{p}_{\mathrm{He}} &= \vec{p}_{\gamma'} + \vec{p}_{\mathrm{He}^{1+}} + \vec{p}_{\mathrm{e}} && (\text{Compton, } \mathrm{He}^{1+}) \\
\vec{p}_\gamma + \vec{p}_{\mathrm{He}} &= \vec{p}_{\gamma'} + \vec{p}_{\mathrm{He}^{2+}} + \vec{p}_{\mathrm{e1}} + \vec{p}_{\mathrm{e2}} && (\text{Compton, } \mathrm{He}^{2+})
\end{aligned}$$

The incoming photon momentum, $\vec{p}_\gamma$, has a value of 2.3 a.u. at 8 keV energy, the momentum of the incoming target atom $\vec{p}_{\mathrm{He}}$ is zero (within the above described properties of the supersonic gas jet). The final state momenta of the scattered photon, the emitted electrons and the recoil ion ($\vec{p}_{\gamma'}$, $\vec{p}_{\mathrm{e}_i}$, $\vec{p}_{\mathrm{He}^{1+,2+}}$) must compensate the incoming photon momentum.

For single ionization by photoabsorption at 8 keV the electron leaves with a momentum of 24 a.u.. Therefore the recoil ion momentum vector given by $\vec{p}_{\mathrm{He}^{1+}} = \vec{p}_{\mathrm{e}} - \vec{p}_\gamma$ ends on a sphere with radius of 24 a.u. shifted forward by $\vec{p}_\gamma$ in the laboratory frame. The recoil ion density distribution on the sphere must reflect the dipolar electron emission pattern due to the linear polarisation of the synchrotron radiation. According to theoretical investigations [22,23]

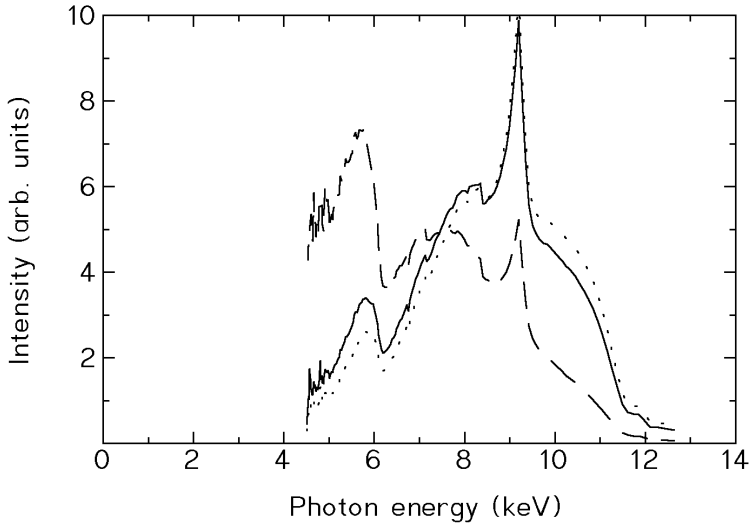

FIGURE 0.2 Full line: photon energy distribution as used in the experiment. Dashed line: photon energy distribution folded with the $E^{-7/2}$ dependence of the He^{1+} photoionization cross section [21,15], dotted line: photon energy distribution folded with calculated Compton scattering cross sections [4,5,7].

higher orders than the dipole portion contribute only with less than 2% in this experiment.

In a Compton scattering process the nucleus acts a spectator, during the ionization process almost no momentum is transfered to the ion. Thus the recoil ion momentum represents essentially that of the nucleus in the initial state which is the compensated target electron momentum distribution. Therefore recoil ions following Compton scattering are expected with small final momenta of about 1 a.u.. Samson et al. have recently used this fact to measure the cross section for He^{1+} production by Compton scattering [24].

RESULTS

The measured momentum distribution of the He^{1+} ions is shown in FIG. 0.3. It is plotted in the p_x-p_y plane, where x is the direction of the electric field vector of the linear polarized light, y is the one of the He gas jet and z is the one of the photon beam. For the geometry see FIG. 0.1. The data of FIG. 0.3 are summed over momenta in z direction –30 a.u. $< p_z <$ 30 a.u. Due to the rotational symmetry of the system the distribution must be symmetrical with respect to the p_x-axis. Ions resulting from the residual He gas atoms can be seen in FIG. 0.3 at $p_y \approx -6$ a.u.

The distinct recoil ion momentum patterns described above can clearly be

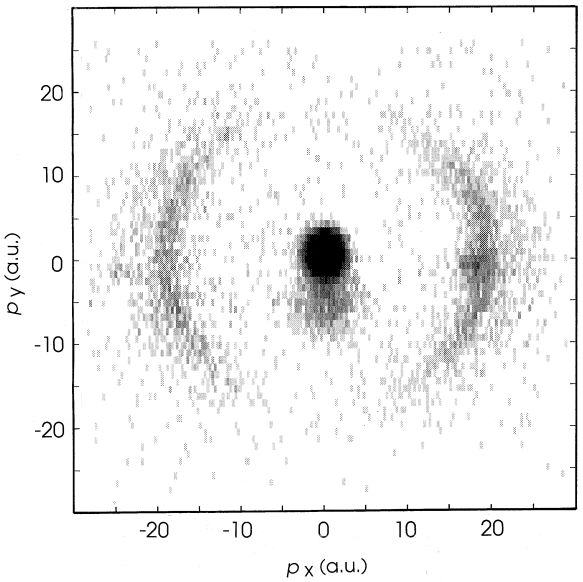

FIGURE 0.3 Measured momentum distribution of He^{1+} ions in the x-y plane, integrated over the momentum in z direction between -30 and 30 a.u.

observed in this spectrum: the one close to zero momentum due to Compton scattering and the distribution along the sphere populated with a dipole distribution pattern from photoabsorption. The larger width of the sphere is mainly due to the energy spread of the incoming photons. The dashed line in FIG. 0.2 represents the photon energy distribution folded with the $E^{-7/2}$ dependence of the photoabsorption cross section [21,15]. After integrating over the full momentum sphere twice as many He^{1+} ions from Compton scattering as from photoabsorption are observed in the experiment. This is in good agreement with the result calculated on the basis of the photon energy distribution and the calculated absolute cross sections for photoabsorption ($\sigma_{\mathrm{Ph}}^{1+}$) and Compton scattering (σ_{C}^{1+}) [4,5,7].

Projections of the full momentum patterns on the x plane for single and double ionization are shown in FIG. 0.4. The He^{2+} momentum distribution is found to be very similar to the one for single ionization. This is in agreement with previous findings that at this high energy the dominant He^{2+} production process for photoabsorption is the emission of one very fast and one slow electron [23].

By integrating over the respective volumes in momentum space we obtain R_C and R_{Ph} separately. The results are given in Table I and displayed in FIG. 0.5. The respective energy is the mean value of the folded photon spectrum (see FIG. 0.2). The horizontal error bars indicate the spectral region from which 67% of all He^{1+} ions originate. Due to the high photon flux the statistical error for R_C is neglectibly small (0.01%). By our technique we are also able to definitely avoid the three major systematical errors of all former

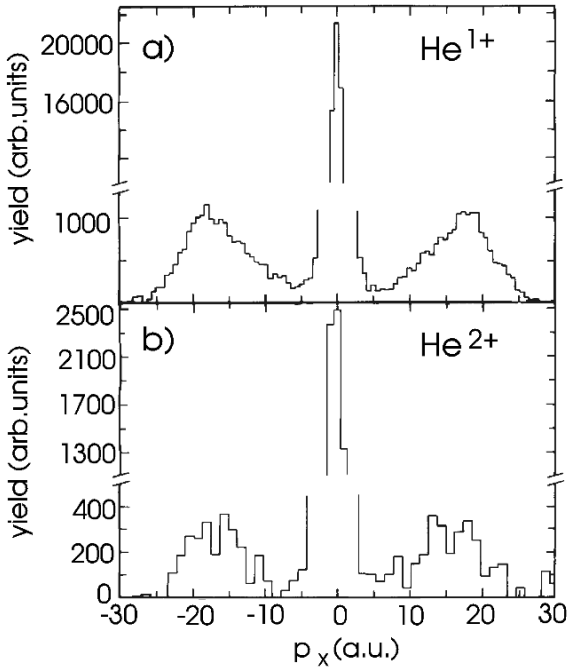

FIGURE 0.4 Measured recoil ion momentum distributions in the x plane. (a) single ionization, (b) double ionization. Intergration over p_z as in FIG. 0.3

high-energy studies, which are small contributions from low-energy stray light, ionization by secondary electrons and charge exchange of the ions with the target gas [11,10]. Low energetic photons would cause photoabsorption and would yield smaller recoil ion momenta. Secondary electrons would not be restricted to the path of the photon beam and therefore result in He ions created along the gas jet and not only at the intersection point with the photon beam, which can be separated with the help of the detector position. The well localized gas jet and the good background pressure of $2 \cdot 10^{-7}$ hPa prevent secondary collisions of the ions resulting in charge exchange. Thus, the only remaining systematical error could be a charge state dependence of the detection efficiency of the channel-plate. This was checked two-fold: First the amplification of the channel-plate was reduced by a factor of two (the pulse height of the channel-plate signal is recorded for each event) by reducing the overall operation voltage by 100 V. Second, measurements were performed with two different postacceleration voltages of 2000V and 1000V.

	Photon energy	$R = \sigma^{2+}/\sigma^{1+}$
Photoabsorption	$7.0^{+2.1}_{-1.6}$keV	1.72±.12%
Compton scattering	$8.8^{+1.5}_{-1.65}$keV	1.22±.06%

TABLE 0.1 Ratios of double to single ionization.

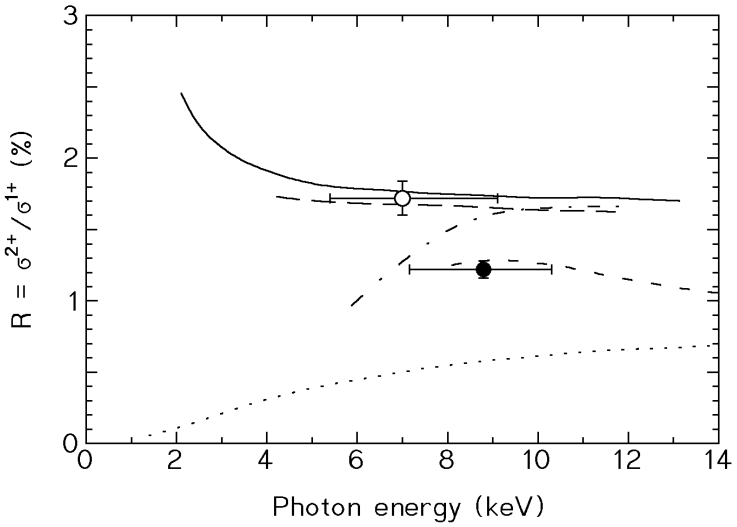

FIGURE 0.5 Ratios of double to single ionization. Full circle: experimental ratio for Compton scattering (R_C), open circle: experimental ratio for photoabsorption (R_{Ph}). The data have been measured with light of an energy distribution as given in FIG. 0.2. The horizontal error bars indicate the energy region from which 67% of all He^{1+} ions result (based on cross sections from [21,4,5,7]). Full line: R_{Ph} from [4], broken line: R_{Ph} from [7], dashed line: R_C from [12], dotted line: R_C from [8], dash-dotted line: R_C from [7].

Both tests yielded the same R_C within 5%. The error given in table I is the sum of our estimate of the systematical error based on these cross checks and the statistical error. The one of R_{Ph} is somewhat larger and mainly due to the background subtraction for the He^{2+} charge state. Ionization of the residual gas was the main contribution for the total recoil ion production, only about 4% of all events result from helium photoabsorption. These counts are distributed over a large volume in momentum space making background subtraction much more difficult than for the Compton effect.

For photoabsorption our experiment is in excellent agreement with the prediction of R_{Ph}=1.67% by different authors [13–15,4]. For Compton scattering our measured ratio is close to the prediction of Andersson and Burgdörfer and we can definitely rule out the values of R_C=0.6% as predicted by Surić et al. [8] and of R_C=1.65% as predicted by Hino et al. [7]. According to theoretical estimates [4] we have already reached the high-energy asymptotic value for R_{Ph}. This result is supported by the value R=(1.6 ± 0.3)% found by Levin et al. [11] at 2.8 keV which agrees with our finding. This value represents only photoabsorption because at this energy the Compton cross section is in the order of 1% of the one for photoabsorption [4]. For Compton scattering the emitted electron energy is still significantly below 500eV and we expect

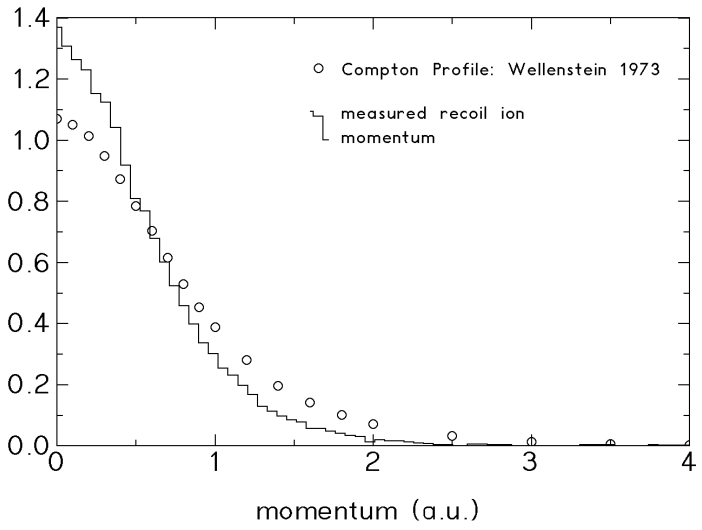

FIGURE 0.6 He^{1+} momentum distribution in the x plane around zero in comparison with the Compton profile [25]. The area under the recoil ion momentum distribution is normalized to that under the Compton profile.

not yet to have reached the asymptotic regime. Therefore, it cannot yet be determined if R_C and R_{Ph} have the same value in the high-energy limit as predicted by Amusia [16].

The He^{1+} momentum distribution in x direction for Compton processes is presented in FIG. 0.6 in an enlarged scale in comparison with the Compton profile [25]. Since in this experiment only the momentum vector of the recoil ion is determined, the value of momentum transfer $K = \vec{p}_{\gamma'} - \vec{p}_{\gamma}$ is not known. Thus, the recoil ion momentum distribution represents the "Compton profile integrated over all momentum transfers K". In particular the included regime of small K will affect the recoil ion momentum distribution. The efficient post collison interaction between the slow ejected electron and the ion will result in a shift of the momentum distribution towards smaller values, as it can be seen in our spectrum. A similar result was found for electron impact [26].

For a further investigation an experiment in the photon energy region from 50 to 100 keV is presently in preparation to reach the asymptotic limit for Compton scattering. A coincident detection of an emitted electron or the scattered photon will allow to determine K and thus provide detailed information on the one-electron Compton profile and, in comparison to this, on the two-electron sum profile after double ionization.

In conclusion, we have experimentally demonstrated that photoabsorption and Compton scattering yield clearly distinct recoil ion momentum distributions. We have exploited this difference in momentum space to experimen-

tally separate the processes for single and double ionization of He at a photon energy of about 8 keV. We find the ratio of double to single ionization by photoabsorption and Compton scattering to be different at this energy.

ACKNOWLEDGMENTS

The work was financially supported by BMFT, DFG, and the EC. These experiments would not have been possible without the patient acceptance of us by the main synchrotron radiation users, namely K. Kjær, G. Brezesinski, L. Leiserowitz, and coworkers. We acknowledge helpful discussion with A. Lahmam-Bennani, C.L. Cocke, J. Burgdörfer, P. Bergstrom, T. Surić, M. Amusia, R. Dreizler, H.J. Lüdde and J.R. Samson. We received indispensable help in building the supersonic gas jet from U. Buck.

REFERENCES

* e-mail: spielberger@ikf.uni-frankfurt.de

1. O. Schwarzkopf et al. *Phys. Rev. Lett.*, 70:3008, 1993.
2. A. Huetz et al. *J. Phys.*, B27:L13, 1994.
3. F. Maulbetsch and J.S. Briggs. *J. Phys.*, B26:L647, 1993.
4. L.R. Andersson and J. Burgdörfer. *Phys. Rev. Lett.*, 71:50, 1993.
5. P.M. Bergstrom, Jr., K. Hino, and J. Macek. *Phys. Rev.*, A51:3044, 1995.
6. J.A.R. Samson, C.H. Green, and R.J. Bartlett. *Phys. Rev. Lett.*, 71:201, 1993.
7. Ken-ichi Hino, P.M. Bergstrom, and J.H. Macek. *Phys. Rev. Lett.*, 72:1620, 1994.
8. T. Surić et al. *Phys. Rev. Lett.*, 73:790, 1994.
9. A. Dalgarno and H.R. Sadeghpour. *Comm. At. Mol. Phys.*, 30:143, 1994.
10. J.C. Levin et al. *Phys. Rev.*, A47:R16, 1993.
11. J.C. Levin et al. *Phys. Rev. Lett.*, 67:968, 1991.
12. L.R. Andersson and J. Burgdörfer. *Phys. Rev.*, A50:R2810, 1994.
13. F.W. Byron and C.J. Joachain. *Phys. Rev.*, 164:1, 1967.
14. T. Åberg. *Phys. Rev.*, A2:1726, 1970.
15. A. Dalgarno and H.R. Sadeghpour. *Phys. Rev.*, A46:R3591, 1992.
16. M. Ya. Amusia and A.I. Mikhailov. *J. Phys.*, B28:1723, 1995.
17. M. Inokuti. *Rev. Mod. Phys.*, 43:297, 1971.
18. J. Ullrich et al. *Comm. At. Mol. Phys.*, 30:285, 1994.
19. R. Dörner et al. *Phys. Rev. Lett*, 72:3166, 1994.
20. V. Mergel et al. *Phys. Rev. Lett*, 20:2200, 1995.
21. T. Ichihara, K. Hino, and J.H. McGuire. *Phys. Rev.*, A44:R6980, 1991.
22. R. H. Pratt and L. LaJohn. private communication.
23. M.Ya. Amusia et al. *J. Phys.*, B8:1247, 1975.
24. J.A.R. Samson et al. *Phys. Rev. Lett.*, 72:3329, 1994.
25. H.F. Wellenstein and R.A. Bonham. *Phys. Rev.*, A7:1568, 1973.
26. O. Jagutzki et al. accepted by *Z. Phys. D*